Multipartite Entanglement Accumulation in Quantum States: Localizable Generalized Geometric Measure

Debasis Sadhukhan, Sudipto Singha Roy, Amit Kumar Pal, Debraj Rakshit, Aditi Sen(De), and Ujjwal Sen
Harish-Chandra Research Institute, Chhatnag Road, Jhunsi, Allahabad - 211019, India and
Homi Bhabha National Institute, Training School Complex, Anushaktinagar, Mumbai 400094, India

Multiparty quantum states are useful for a variety of quantum information and computation protocols. We define a multiparty entanglement measure based on local measurements on a multiparty quantum state, and an entanglement measure averaged on the post-measurement ensemble. Using the generalized geometric measure as the measure of multipartite entanglement for the ensemble, we demonstrate, in the case of several well-known classes of multipartite pure states, that the localized multipartite entanglement can exceed the entanglement present in the original state. We also show that measurement over multiple parties may be beneficial in enhancing localizable multipartite entanglement. We point out that localizable generalized geometric measure faithfully signals quantum critical phenomena in well-known quantum spin models even when considerable finite-size effect is present in the system.

I. INTRODUCTION

Emergence of multipartite entanglement [1] as a crucial ingredient in several information processing tasks like measurement-based quantum computation [2], quantum dense coding [3–5], and quantum cryptography [6–8] has emphasized the importance of quantifying entanglement in multipartite systems. Multipartite entanglement has been proven essential also in detecting cooperative phenomena such as quantum phase transitions (QPTs) [9, 10], and to explain transport properties in photosynthetic complexes [11] (see [12–14] for reviews). In this respect, it has also been pointed out that multipartite entanglement can be necessary to detect some QPTs, which are not clearly signaled by bipartite measures [15]. The growing interest for estimating multipartite entanglement in many-body systems is also sustained by impressive experimental advances towards creating entangled particles in laboratories with various substrates, *e.g.*, trapped ions [16], photons [17], superconducting materials [18], nuclear magnetic resonance (NMR) [19], and optical lattices [20] (see also [21]). However, despite considerable attempts, progress in developing measures of multipartite entanglement has been limited [1, 10, 22–31].

An interesting utility of multipartite quantum states is the measurement based quantum computation [2], where quantum gates are implemented by solely performing suitable measurements on different local parts of a previously prepared quantum state of a number of parties, eg., on a lattice. In a different situation, one may consider performing measurements on some parts of a multiparty quantum state, so that the remaining parties share a useful quantum state. A particularly important example is provided by the Greenberger-Horne-Zeilinger (GHZ) state [32], given by $|\psi\rangle = (|0\rangle^{\otimes N} + |1\rangle^{\otimes N})/\sqrt{2}$. Tracing out m qubits from $|\psi\rangle$, where $m < N-1$, leads to a separable state with vanishing entanglement, while performing local measurements over the m parties, one obtains an ensemble of pure states conditioned to the measurement outcomes, which has non-zero entanglement. Such protocols encourages one to consider a general scenario where an N-party quantum state, ρ_N, is measured at a certain number of parties, to obtain an ensemble of a lower number of parties, with the measurements being so chosen that the average entanglement, according to a pre-decided measure, of the post-measurement ensemble is maximized. Such entanglement accumulation scheme have been previously used to define entanglement measures [33–36], where it was usual to choose the number of unmeasured parties as two. Here we go beyond the regime, where the number of parties in the post-measurement ensemble is more than two.

In this paper, we introduce a localizable multipartite entanglement (LME) measure, in terms of the geometric measures of entanglement [10, 27, 30], and discuss its various properties. Specifically, we prove that the LME is invariant under local unitary transformations, and show that it is bounded above by any upper bound of its parent multiparty entanglement measure. Note that the concept of LME requires the knowledge of another multiparty entanglement measure, and due to the compact computational form of multiparty entanglement, as quantified by the generalized geometric measure (GGM) [10, 27, 30], we restrict ourselves to the cases in which the GGM is identified with the latter measure. We call the corresponding quantity as the localizable GGM (LGGM). For arbitrary number of qubits, we analytically find the exact expression of LGGM for several classes of multipartite states which include the generalized GHZ (gGHZ) state [32], generalized W (gW) state [35, 37, 38], and Dicke states with different excitations [39–41], when measurement is restricted to a single qubit. Interestingly, we find that in the case of gGHZ state, LGGM coincides with the GGM of the original state. On the other hand, for gW state, local measurement helps to accumulate higher multipartite entanglement in the lower number of qubits, as compared to the content of multipartite entanglement of the original state, showing qualitatively distinct behavior than the gGHZ state. Moreover, we prove that the value of LGGM over two qubits in the case of an arbitrary three-qubit pure state is always lower bounded by the value of the geometric measure of the original state, while no such bound exists when higher number of qubits are involved.

For specific classes of four- and five-qubit states, we show that local measurement on two parties may help to increase LGGM, as compared to the same with only single-qubit measurement. Extensive numerical simulations seem to imply that such observation holds for almost all four- and five-qubit states. We also consider the utility of LGGM in detecting quantum cooperative phenomena in many-body systems. We perform finite-size calculations to show that it can detect the QPTs [42] occurring in the one-dimensional (1d) quantum Ising model in a transverse

field [43]. Moreover, we show that LGGM signals the QPTs including the Kosterlitz-Thouless (KT) transition of the 1d XXZ model [44–47].

The paper is organized as follows. Sec. II contains the formal definition of LME using geometric measures as the quantifier. It also describes various properties of LME. Sec. III A describes the results regarding single-qubit measurement in the case of several well-known examples of multiqubit states, such as the generalized GHZ state (gGHZ), the generalized W (gW) state, and the N-qubit symmetric states. The effect of measurement over more than one qubit on the value of LME, along with specific examples in the case of four- and five-qubit systems, is discussed in Sec. III B. The numerical results regarding arbitrary three-, four-, and five-qubit pure states are presented in Sec. III C. Sec. IV deals with the study of the behavior of LME in well-known quantum spin models. Sec. V contains the concluding remarks.

II. LOCALIZABLE MULTIPARTITE ENTANGLEMENT

In this section, we formally introduce the LME, and discuss its properties.

A. Definition

The LME of a multiparty pure state can be defined as the maximum average multipartite entanglement that can be concentrated over a certain specified set of parties in the system by performing local measurements over the rest of the parties. Let us consider a pure state $|\Phi_N\rangle$, which describes a multipartite system consisting of N parties distinguished by the index $i = 1, 2, \cdots N$. For simplicity, while defining the LME, we consider that the dimension of Hilbert space of each of the parties is same, i.e., $d_i = d$, $i = 1, \cdots, N$. However, a more generalized definition using different dimensions for different parties can also be given.

Let us consider local quantum measurements performed by any m parties on the N-party state, $|\Phi_N\rangle$. Let $\mathbf{r}$ be the set of positions of the measured qubits, given by $\mathbf{r} = \{r_j\}, j = 1, \cdots, m$, where $r_j \in \{1, 2, \cdots, N\}$. The local measurements lead to a post-measurement outcome ensemble, $\{p^l, |\Psi_N^l\rangle\}$, of pure states. The index l denotes the running index of the measurement outcomes, and runs over the joint Hilbert space of the measured parties having dimension d^m. Here, p^l is the probability of obtaining the state $|\Psi_N^l\rangle = M^l|\Phi_N\rangle$, with M^l being the corresponding measurement operator, and $\sum_{l=1}^{d^m} p^l = 1$. The LME for the multipartite state $|\Phi_N\rangle$, for local measurements at $\mathbf{r}$, can be defined as

$$E_{L,\mathcal{E}}^{n,\mathbf{r}}(|\Phi_N\rangle) = \sup_{\mathcal{M}} \sum_{l=1}^{d^m} p^l \mathcal{E}\left(|\psi_n^l\rangle\right), \tag{1}$$

where $\mathcal{M} \equiv \{M^l\}$ is a set of measurement operators on the d^m-dimensional Hilbert space, and $\mathcal{E}\left(|\psi\rangle\right)$ is an arbitrary multipartite entanglement measure for the state $|\psi\rangle$. Here, $n = N - m$ ($n \leq N - 1$), and is currently redundant in the notation. Its use will become clear once we reach Eq. (3). We will also assume that $n \geq 2$, although the formalism adopted here can be generalized to the case of $n = 1$ also. The state $|\psi_n^l\rangle$ corresponding to the N-party state $|\Psi_N^l\rangle$, for a fixed $\mathbf{r}$ and a fixed measurement outcome l, is obtained by tracing out the m parties of which local measurements are performed. The tracing out operation is performed after the local measurement has been carried out. The supremum is taken over all complete sets of measurement operators in $\mathcal{M}$, since the supremum is not guaranteed to be attained within the set, due to the possible complex nature of $\mathcal{M}$.

It is important to note here that the conceptualization of an LME depends on the understanding of another measure of multiparty entanglement of a lower number of parties. This latter measure is in some sense acting as a "seed measure" for the LME. To define LME, one may consider measurement protocols corresponding to, for example, projective measurements (PV) without classical communication between the parties, or positive operator valued measures (POVMs) without classical communication between the parties, or general local operations and classical communication (LOCC). In the last case, the classical communication (CC) is among the m parties over which the local operations are performed. It is clear that

$$E_{L,\mathcal{E}}^{n,\mathbf{r}}|_{\text{PV}} \leq E_{L,\mathcal{E}}^{n,\mathbf{r}}|_{\text{POVM}} \leq E_{L,\mathcal{E}}^{n,\mathbf{r}}|_{\text{LOCC}}, \tag{2}$$

for a fixed multipartite state, $|\Phi_N\rangle$, a fixed set of measured parties, $\mathbf{r}$, and a chosen multiparty entanglement measure, $\mathcal{E}$.

One must note here that for a fixed initial multipartite state $|\Phi_N\rangle$, and a fixed set of measurement protocols, the value of LME depends on two factors: **(i)** the multipartite entanglement measure $\mathcal{E}$ (the seed measure), and **(ii)** the set $\mathbf{r}$, i.e., the choice of m parties over which local measurements are performed. Before discussing the choice of $\mathcal{E}$, let us briefly consider the dependence of LME over the set $\mathbf{r}$ that is inherent in the definition. For an N-partite system with local measurements at m parties, a set $\mathbf{R} = \{\mathbf{r}_\alpha\}$, $\alpha = 1, 2, .., \binom{N}{m}$, of all possible choices of $\mathbf{r}$ exists, thereby allowing $\binom{N}{m}$ number of values of LME, $E_{L,\mathcal{E}}^{n,\mathbf{r}_\alpha}$. Therefore, the LME, $E_{L,\mathcal{E}}^{n,\mathbf{r}_\alpha}$, is "local" in the sense that it changes with the choice of the set $\mathbf{r}_\alpha$. In light of this fact, one can also define a "global" value of the LME for a multipartite state with fixed values of N and m as

$$E_{GL,\mathcal{E}}^{n} = \max_{\mathbf{R}} \{E_{L,\mathcal{E}}^{n,\mathbf{r}_\alpha}\}. \tag{3}$$

Note that if the initial state $|\Phi_N\rangle$ is a symmetric state, such maximization over $\mathbf{R}$ is not required. Note also that the relative positions of the parties labeled by "$\mathbf{r}_\alpha$", for a specific α, with respect to each other as well as the rest of the parties does not affect the value of LME. From now on, without any loss of generality, we assume that the measurements are performed at $r_j = j$, $j = 1, 2, \cdots, m$, while $|\psi_n^l\rangle$ denotes the state of the remaining n parties.

This definition can be extended to an arbitrary mixed state when the input state is an N-party state $\varrho_{1,2,\cdots,N}$, and the measurement is performed on any m parties. The problem in this case remains with the choice of a computable multipartite entanglement measure $\mathcal{E}$, which is defined for the mixed states. Although the notion of entanglement measures in multipartite systems is an active field of research, the number of such computable measures, even in the case of the pure states, is still limited. Another avenue to extend the LME to mixed states is

via the convex-roof optimization. Convex-roof optimization is, however, typically difficult to perform, and has been successful in only a few instances. See [48] for examples within quantum information.

Reverting back to the case of pure states, in principle, an LME can be defined by using any one of the known candidates for pure state multipartite entanglement measure as the seed measure, such as relative entropy of entanglement [22], global entanglement [23], and other multipartite measures [1, 24]. However, in the present study, we focus on geometric measures (GM) of entanglement [1, 9, 10, 25–28] for multipartite pure states. More specifically, we use the "K-separability based GM" (K-GM) to discuss the properties of the LME. For the purpose of computation, we choose the generalized geometric measure (GGM), which is computable for a multiparty pure state in arbitrary dimensions and for arbitrary number of parties. Short descriptions of these measures can be found in Appendix A.

In this paper, we have confined ourselves to consideration of measurements that are local. It is possible to define a multipartite entanglement measure for which non-local measurements are allowed in the optimization. However, non-local measurements, even if performed on two parties at a time, can generate genuine multiparty entanglement, and therefore will result in difficulties in defining the monotonicity of the so-obtained measure under LOCC. Furthermore, parametrization of the non-local measurements via entangled bases require a large number of parameters that increase exponentially with the increase in the number of parties measured.

B. Properties

We now prove several properties of LME. We use K-GM as the multipartite entanglement measure, and local projective measurements, in which case, Eq. (1) reads

$$E_L^{n,\mathbf{r}_\alpha}(|\Phi_N\rangle) = \sup_{\mathcal{P}} \sum_{l=1}^{d^m} p^l G_K\left(|\psi_n^l\rangle\right), \tag{4}$$

where $\mathcal{P} \equiv \{P^l\}$ denotes a complete set of local projectors acting on the parties distinguished by $\mathbf{r}_\alpha$. From now onward, we discard the index $\mathcal{E}$. We start by looking into the bounds of the measure, which leads us to the following theorem.

Theorem 1. *For an arbitrary state $|\Phi_N\rangle$ describing a quantum system of N parties, $0 \leq E_L^{n,\mathbf{r}_\alpha} \leq g$, where $G_K \leq g$.*

Theorem 1 provides an upper bound of LME depending on the choice of the seed measure, provided an upper bound is known for the seed. Corollary 1.1 follows directly from Theorem 1, and the definition of E_{GL}^n (Eq. (3)).

Corollary 1.1. *For an arbitrary state $|\Phi_N\rangle$ describing a quantum system of N parties, $0 \leq E_{GL}^n \leq g$, where $G_K \leq g$.*

Note that for $K = 2$, $G_K \equiv \mathcal{G}$ for an N-qubit system, and the above property implies $E_L^{n,\mathbf{r}_\alpha} \leq 1/2$, since $\mathcal{G} \leq 1/2$. Our next theorem is on the effect of local unitary (LU) operations on LME.

Theorem 2. *$E_L^{n,\mathbf{r}_\alpha}$ remains invariant under local unitary transformations.*

To determine the criteria for vanishing $E_L^{n,\mathbf{r}_\alpha}$, we intend to characterize the set of multipartite states, $\{|\Phi_N\rangle\}$, for which $E_L^{n,\mathbf{r}_\alpha} = 0$. We first consider the following theorem.

Theorem 3. *For a K-separability based GM, a non-zero value of $E_L^{n,\mathbf{r}_\alpha}$ for an N-partite pure state, $|\Phi_N\rangle$, is possible with $n = N - m$, m being the number of parties in which measurement is performed, only when the separability, M, of the original state is such that $1 \leq M \leq K + m - 1$.*

Proof. To prove the above theorem, let us first assume that the N-partite system is composed of two partitions denoted by A, and B. The first one consists of the m parties over which local measurements are performed, while the rest $n = N - m$ parties construct the partition B. For the value of $E_L^{n,\mathbf{r}_\alpha}$ to be non-zero, at least one of the states, $\{\psi_n^l\}$, of the post-measurement ensemble consisting of d^m states must not be K-separable, so that $G_K(|\psi_n^l\rangle) \neq 0$. This implies that the state $|\psi_n^l\rangle$ is allowed to be K'-separable, where $1 \leq K' \leq K - 1$. Moreover, irrespective of whether the partitions A and B share entanglement among each other, the possible separability of the partition A consisting of m parties dictates that the original state, $|\Phi_N\rangle$, is allowed to be $(K' + j)$-separable, where $1 \leq j \leq m$. Combining these two results, one obtains the allowed range of M as 1 to $K + m - 1$. ∎

All the characteristics of LME discussed above remains unchanged if K-GM is replaced by GGM as the genuine multipartite entanglement measure.

III. LGGM IN MULTIPARTY QUANTUM STATES

A. Single-qubit measurement: LGGM vs. GGM

Let us consider an N-party pure state in $(\mathbb{C}^2)^{\otimes N}$. The local projective measurement, $\mathcal{P}$, on a qubit j ($j = 1, 2, \cdots, N$), can be represented by a complete set of rank-1 projectors, $\{\Pi_j^l\}$, such that $\Pi_j^l = |\xi_j^l\rangle\langle\xi_j^l| \otimes \mathbb{I}_{N-1}$, $l = 1, 2$, is given by

$$\begin{aligned} |\xi_j^1\rangle &= c_{\theta_j/2}|0\rangle + e^{i\phi_j} s_{\theta_j/2}|1\rangle, \\ |\xi_j^2\rangle &= -s_{\theta_j/2} e^{-i\phi_j}|0\rangle + c_{\theta_j/2}|1\rangle, \end{aligned} \tag{5}$$

with $0 \leq \theta_j \leq \pi$, $0 \leq \phi_j < 2\pi$, and c_x and s_x stand for $\cos x$ and $\sin x$ respectively. Here, $\mathbb{I}_{N-1}$ is the identity operator in the Hilbert space of the $N-1$ qubits, and $\{|0\rangle, |1\rangle\}$ is the computational basis in the qubit Hilbert space. In this representation, the supremum involved in the definition of LME is obtained by performing a maximization over the space of the real parameters, (θ_j, ϕ_j). If local measurements are performed over a collection of qubits denoted by $\mathbf{r} \equiv \{r_j\}$, $j = 1, 2, \cdots, m$ with $m > 1$, the supremum has to be obtained over a total of $2m$ real parameters, $(\theta_{r_j}, \phi_{r_j})$. Using GGM as the seed measure, Eq. (1) takes up a simpler form, given by

$$E_L^r = \sup_{\mathcal{P}} \sum_{l=1}^{2} p^l \mathcal{G}(|\psi_{N-1}^l\rangle). \tag{6}$$

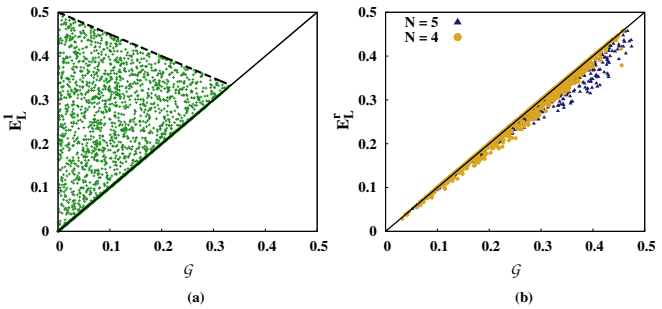

FIG. 1. (Color online.) (a) Plot of E_L^1 vs. $\mathcal{G}$ for three-qubit gW states. To obtain the scatter diagram, 10^5 three-qubit gW states are generated Haar-uniformly. The solid line represents the line $E_L^1 = \mathcal{G}$, while the dashed line correspond to $2E_L^1+\mathcal{G} = 1$. (b) Plot of E_L^1 vs. $\mathcal{G}$ in the case of Haar-uniformly generated generalized superposition of Dicke states, as given in Eq. (10). To obtain the scatter diagram, 10^5 states of the form $|D_g^N\rangle$ are generated Haar-uniformly for each of the cases $N = 4$ and $N = 5$. All quantities plotted in both figures are dimensionless.

#	Ordering	$\mathbf{E_L^1}$	$\mathbf{E_L^2}$	$\mathbf{E_L^3}$	$\mathcal{G}$	Partition
1	$\|a_1\|^2 \geq \|a_2\|^2 \geq \|a_3\|^2$	$\|a_2\|^2$	$\|a_3\|^2$	$\|a_3\|^2$	$\|a_3\|^2$	1:23
2	$\|a_1\|^2 \geq \|a_3\|^2 \geq \|a_2\|^2$	$\|a_2\|^2$	$\|a_3\|^2$	$\|a_2\|^2$	$\|a_2\|^2$	2:13
3	$\|a_2\|^2 \geq \|a_1\|^2 \geq \|a_3\|^2$	$\|a_1\|^2$	$\|a_3\|^2$	$\|a_3\|^2$	$\|a_3\|^2$	1:23
4	$\|a_2\|^2 \geq \|a_3\|^2 \geq \|a_1\|^2$	$\|a_1\|^2$	$\|a_1\|^2$	$\|a_3\|^2$	$\|a_1\|^2$	3:12
5	$\|a_3\|^2 \geq \|a_1\|^2 \geq \|a_2\|^2$	$\|a_2\|^2$	$\|a_1\|^2$	$\|a_2\|^2$	$\|a_2\|^2$	2:13
6	$\|a_3\|^2 \geq \|a_2\|^2 \geq \|a_1\|^2$	$\|a_1\|^2$	$\|a_1\|^2$	$\|a_2\|^2$	$\|a_1\|^2$	2:13

TABLE I. Different orderings of $\{|a_1|^2, |a_2|^2, |a_3|^2\}$ and corresponding values of E_L^r ($r = 1, 2, 3$), and $\mathcal{G}$ in the case of three-qubit gW state. For all orderings, $E_L^1 \geq \mathcal{G}$. The last column shows the bipartition from which the maximum Schmidt coefficient is obtained.

Note that in Eq. (6), we have discarded the superscript n since it has a constant value $n = N - 1$ in the present case. To keep the notations uncluttered, we also replace $\mathbf{r}_\alpha$ with the position index, r, since r can now have N possible values, i.e., $r = 1, 2, \cdots, N$. In this section, and in the rest of the paper, unless otherwise stated, we always consider local measurement over the first qubit of the system in the case of a single-qubit measurement.

Generalized GHZ state. The first example that we consider is the N-qubit gGHZ state, given by [32] $|GHZ_N\rangle_g = a_1|0\rangle^{\otimes N} + a_2|1\rangle^{\otimes N}$, where a_1 and a_2 are complex numbers with $|a_1|^2 + |a_2|^2 = 1$. Without any loss of generality, let us assume that $|a_1|^2 \geq \frac{1}{2} \geq |a_2|^2$. Since $|GHZ_N\rangle_g$ is symmetric under swapping of parties, $E_L^r = E_L$ for $r = 1, 2, \cdots, N$. The following proposition is for the LGGM of N-qubit gGHZ states (see Appendix B for the proof).

Proposition I. *For the N-qubit gGHZ state, $E_L^1 = \mathcal{G}$.*

The value of LGGM remains unchanged in the case of the gGHZ state if measurement is performed over a higher number of qubits ($m > 1$). However, in subsequent discussions, we shall be providing examples of multipartite quantum states for which the situation is different. As a special case of the N-qubit gGHZ state, the LGGM for the GHZ state ($a_1 = a_2 = 1/\sqrt{2}$) of N qubits can be obtained as $E_L^1 = 1/2$.

Generalized W state. Our next example is the N-qubit gW state, given by [35, 37, 38] $|W_N\rangle_g = \sum_{i=1}^N a_i|0\rangle^{\otimes(i-1)}|1\rangle_i|0\rangle^{\otimes(N-i)}$, where $\{a_i\}$, $i = 1, 2, \cdots, N$, are complex numbers such that $\sum_{i=1}^N |a_i|^2 = 1$. Note that unlike the gGHZ state, the gW state is not symmetric under swapping of parties, which leads to a collection of N values of LGGM, $\{E_L^r\}$, $r = 1, 2, \cdots, N$. The GGM of the state, in the present case, is given by $\mathcal{G} = \min\{|a_i|^2\}$, where $i = 1, 2, 3$. For the purpose of demonstration, we start with the case of $N = 3$, for which the relation between E_L^r and $\mathcal{G}$ is given by the following proposition (see Appendix B for the proof).

Proposition II. *For an arbitrary three-qubit gW state, $E_L^r \geq \mathcal{G}$ for all values of r.*

The following corollary regarding the lower bound of the "global" LGGM, as defined in Eq. (3), can be obtained directly from Proposition II.

Corollary II.1. *For the tripartite gW state, the global LGGM, $E_{GL} \geq \mathcal{G}$.*

In the case of N-qubit gW states with $N > 3$, the situation is more involved. The difficulty in determining the values of GGM of the states $|\psi^l\rangle$ in the post-measurement ensemble, which now correspond to $N-1$ qubits or less, makes analytical optimization of LGGM rather difficult. However, motivated by the Proposition II, we intend to check whether such a lower bound of LGGM exists if one considers an N-qubit gW state, when measurement is performed only on a single qubit. This leads us to Proposition III. The proof of the Proposition is given in Appendix B.

Proposition III. *For an arbitrary gW state of N-qubits, $E_L^r \geq \mathcal{G}$ for all values of r, provided measurement is performed only on a single qubit.*

Our numerical analysis suggests that irrespective of the value of N, the maximization involved in LGGM for the gW states, is obtained when the local projective measurement is performed in the computational basis, $\{|0\rangle, |1\rangle\}$. Using this information, an upper bound for E_L^r of the state $|W_N\rangle_g$ can also be proved, as given in Proposition IV (see Appendix B for the proof).

Proposition IV. *For an arbitrary N-qubit gW state, E_L^r, for all values of r, is bounded above by the LGGM of the gW state having the same value of $\mathcal{G}$, but with squared modulus of all the coefficients except one, denoted by $|a_i|^2$, being equal to $|a_j|^2 = (1 - |a_i|^2)/(N - 1)$, where $|a_i|^2 = \min\{|a_k|^2\}$, $k = 1, 2, \cdots, N$, $j \neq i$, and $i, j \in \{1, 2, \cdots, N\}$.*

Fig. 1(a) depicts the scatter diagram of E_L^1 vs. $\mathcal{G}$ in the case of a set of 10^5 Haar-uniformly generated three-qubit gW states. The solid line, representing $E_L^1 = \mathcal{G}$, depicts the lower bound of E_L^1 (Proposition II), while the dashed line, representing $2E_L^1 + \mathcal{G} = 1$, correspond to the upper bound given in Proposition IV. Note that all the points in the scatter diagram are enclosed by these two lines, and $\mathcal{G} = 0$. The W state, $|W\rangle$, is obtained from the gW state with $a_i = 1/\sqrt{N}$, $i = 1, 2, \cdots, N$. Evidently, the GGM and LGGM of the W state are equal to each other, having a value $1/N$.

Considering that LGGM of the N-qubit gW state is maximized when measurement is performed in $\{|0\rangle, |1\rangle\}$, we make the following observation.

Observation. For an N-qubit gW state, $E_L^r \geq \mathcal{G}$ if the value of $\mathcal{G}$ is obtained from r:rest bipartition, while in all other cases, $E_L^r = \mathcal{G}$.

We demonstrate the implications of the above observation in Table I, where the E_L^r of three-qubit gW states in different cases (as distinguished by the different orderings of the $|a_i|^2$), are tabulated along with their GGMs. Note that the global LGGM, E_{GL}, is obtained when local projective measurement is performed on the qubit r such that the maximum Schmidt coefficient is obtained from the bipartition r:rest, as presented in the last column. From the table, it is clear that the value of $E_L^{r'}$, when the r':rest bipartition does not provide the maximal Schmidt coefficient, is always equal to the GGM of the three-qubit gW state, which is in agreement with the observation. We shall be investigating this issue, and its possible generalization, while discussing the LGGM of arbitrary three-qubit pure states, in Sec. III C.

Symmetric States. We next consider a special class of multipartite quantum states known as the "symmetric states", which remains unaltered with the permutation of parties. First, we investigate the behavior of LGGM in a special subset of symmetric states – the highly entangled N-qubit Dicke states [39, 40] – with high applicational advantages [41]. An N-qubit Dicke state with k excitations can be represented as

$$|D_k^N\rangle = \frac{1}{\sqrt{\binom{N}{k}}} \sum_i \mathcal{P}_i \left(|0\rangle^{\otimes N-k} \otimes |1\rangle^{\otimes k}\right), \tag{7}$$

where the summation is over all possible permutations of N-qubit product states composed of $N-k$ qubits in the ground state, $|0\rangle$, and the rest k qubits in the excited state, $|1\rangle$. Note that the N-qubit W state can be identified as $|D_1^N\rangle$. The GGM of $|D_k^N\rangle$, with $N > 2$, can be obtained as [40]

$$\mathcal{G} = \begin{cases} \frac{N-2}{2(N-1)} \text{ for } k = \frac{N}{2}, \\ \frac{k}{N} \text{ for } k < \frac{N}{2}. \end{cases} \tag{8}$$

To determine E_L^r, $r = 1, \cdots, N$, of the Dicke state, one has to perform a rank-1 projective measurement on any one of the qubits. The details on the post-measurement ensemble and determination of GGM can be found in Appendix C. We perform extensive numerical analysis for different values of N and k to find that irrespective of the number of qubits and the number of excitations, the optimization of LGGM for $|D_k^N\rangle$ always takes place at $\theta = 0, \phi = 0$, i.e., at the $\{|0\rangle, |1\rangle\}$ basis. The LGGM, in that case, can be obtained as explicit functions of N and k, as

$$E_L^r(\text{even } N) = \begin{cases} \frac{N-2}{2(N-1)} \text{ for } k = \frac{N}{2}, \\ \frac{k}{N} \text{ for } k < \frac{N}{2}. \end{cases}$$

$$E_L^r(\text{odd } N) = \begin{cases} \frac{k}{N} \text{ for } k < \frac{N-1}{2}, \\ \frac{N-1}{2N} - \frac{N+1}{4N(N-2)} \text{ for } k = \frac{N-1}{2}, N > 3, \\ \frac{1}{3} \text{ for } k = 1, 2 \text{ and } N = 3. \end{cases} \tag{9}$$

From Eqs. (8) and (9), it is evident that for $N > 3$, $E_L^r < \mathcal{G}$ for odd N with $k = (N \pm 1)/2$, while in all other cases, $E_L^r = \mathcal{G}$, thereby suggesting an upper bound of LGGM, given by $E_L^r \leq \mathcal{G}$ for symmetric Dicke states of N qubits with k excitations provided the maximization is obtained in the computational basis.

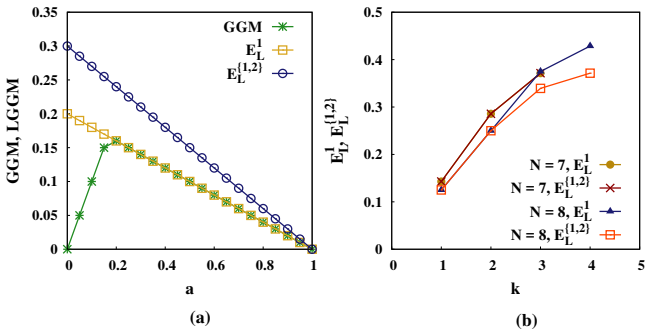

FIG. 2. (Color online.) **(a)** Plot of $\mathcal{G}$, E_L^1, and $E_L^{\{1,2\}}$ as functions of a in case of the four-qubit gW state $|W^4\rangle_g$ with $a_1 = a$, $a_2 = \sqrt{(1-a^2)/5}$, $a_3 = \sqrt{3(1-a^2)/10}$, and $a_4 = \sqrt{(1-a^2)/2}$. **(b)** Plot of E_L^1 and $E_L^{\{1,2\}}$ with k for $N = 7$ and $N = 8$ in the case of Dicke states. All quantities plotted are dimensionless.

A general form of N-qubit symmetric states can be constructed by making superposition of all the Dicke states. Such a state can be written as

$$|D_g^N\rangle = \sum_{k=0}^{N} a_k |D_k^N\rangle, \tag{10}$$

with complex $\{a_k\}$ such that $\sum_{k=0}^{N} |a_k|^2 = 1$. Here, the summation index, k, denotes the possible number of excitations in a Dicke state, and can have values $0 \leq k \leq N$. The difficulty in computing the GGM of an N-qubit symmetric state of the form given in Eq. (10) restricts one to calculate the LGGM of such states only numerically. Our numerical analysis suggests that for $N = 3$, $E_L^1 = \mathcal{G}$, while the upper bound, $E_L^r \leq \mathcal{G}$ holds in the case $N = 4, 5$, like in the case of Dicke states. Fig. 1(b) depicts the variation of E_L^r against $\mathcal{G}$ for 10^5 randomly chosen symmetric states for each of the cases $N = 4$, and 5, where the upper bound is satisfied. For $N = 4$, and 5, the percentage of states for which $E_L^r < \mathcal{G}$ are 33.4%, and 46.8%, respectively, while for the rest of the states, $E_L^r = \mathcal{G}$, up to four decimal places.

B. Can local measurement over more than one qubit be beneficial?

In this section, we focus on the question as to whether increasing the number of measured parties can help to increase localizable entanglement, and discuss examples of multipartite entangled states in this context. To begin with, we point out that in the case of N-qubit gGHZ state, $E_L^r = E_L^{\mathbf{r}_\alpha}$, where $\mathbf{r}_\alpha = \{r_j\}$, $j = 1, 2, \cdots, m$, and $1 < m \leq N-2$. This implies that LGGM does not depend on the number of measured qubits for the gGHZ state. The situation, however, can be drastically different if one considers the gW state of N qubits. As an example, we consider the case of a four-qubit gW state, where the coefficients $\{a_i\}$, $i = 1, \cdots, 4$, are real, such that $a_1 = a$, $a_2 = \sqrt{(1-a^2)/5}$, $a_3 = \sqrt{3(1-a^2)/10}$, and $a_4 = \sqrt{(1-a^2)/2}$. For this state, $\mathcal{G} < E_L^1 < E_L^{\{1,2\}}$ with $a \leq 0.17$, while $\mathcal{G} = E_L^1 < E_L^{\{1,2\}}$ when $a > 0.17$ (Fig. 2(a)), thereby indicating an advantage

State	$\mathcal{G}$	$\mathbf{E_L^1}$	$\mathbf{E_L^2}$	$\mathbf{E_L^3}$	$\mathbf{E_L^4}$	$\mathbf{E_L^{\{1,2\}}}$	$\mathbf{E_L^{\{1,3\}}}$	$\mathbf{E_L^{\{1,4\}}}$	$\mathbf{E_L^{\{2,3\}}}$	$\mathbf{E_L^{\{2,4\}}}$	$\mathbf{E_L^{\{3,4\}}}$
$\|\Psi_7^4\rangle$	1/4	1/4	1/4	1/4	1/4	1/4	1/4	1/4	1/4	1/4	1/4
$\|\Psi_8^4\rangle$	1/4	1/2	1/4	1/4	1/4	1/2	1/2	1/2	1/2	1/2	1/4
$\|\Psi_9^4\rangle$	0	1/2	0	0	0	1/2	1/2	1/2	1/2	1/2	0

TABLE II. The values of $\mathcal{G}$, E_L^r ($r = 1, 2, 3, 4$), and $E_L^{\{r_1,r_2\}}$ ($r_1 \neq r_2$, $r_{1,2} \in \{1, 2, 3, 4\}$) for the four-qubit states $|\Psi_7^4\rangle$, $|\Psi_8^4\rangle$, and $|\Psi_9^4\rangle$.

of measuring more than one qubit. Such instances can also be found in four-qubit states other than gW states, and in quantum states involving higher number of parties (for such examples, see Appendix D). On the contrary, there exist quantum states, for example, N-qubit Dicke states, for which $E_L^{\{1,2\}}$ is not beneficial compared to E_L^1. We determine the values of E_L^1 and $E_L^{\{1,2\}}$ in the case of $|D_k^N\rangle$ with $4 \leq N \leq 10$, for different allowed values of k, and find that irrespective of the value of N and k, $E_L^{\{1,2\}} \leq E_L^1 \leq \mathcal{G}$. The variations of $\mathcal{G}$, E_L^1, and $E_L^{\{1,2\}}$ against different values of k for $N = 7$ and 8 are shown in Fig. 2(b), while the variations of E_L^1 and $E_L^{\{1,2\}}$ with varying k, for $N = 9$ and 10, are qualitatively similar to that for $N = 7$ and 8 respectively. The question of whether this is a generic property of the symmetric states is discussed in the next section. One must note that there exists multiparty states other than Dicke states, for which local measurement over more than one qubit may not be advantageous, as discussed in the next section.

C. Arbitrary N-qubit pure states: Numerical Results

We now consider arbitrary N-qubit pure states, and compare advantages of multi-qubit measurements over single-qubit ones via numerical analysis. We focus on N-qubit pure states with $N = 3, 4$ and 5, and consider different classes of such states. Unless otherwise stated, we Haar-uniformly generate 10^5 arbitrary pure states in each case, and compute $\mathcal{G}$ for the original state, E_L^1, and $E_L^{\{1,2\}}$ in the case of each N-qubit state. In our numerical analysis, the values of two quantities are considered to be equal when they are same upto four decimal places.

In the three-qubit scenario, we separately consider arbitrary three-qubit pure states belonging to the paradigmatic GHZ and the W classes [38] (see Appendix E for a short description of the classes, and the post-measurement ensembles), which are mutually disjoint sets that together construct the entire set of three-qubit pure states. We find that for an arbitrary three-qubit pure state, $E_L^1 \geq \mathcal{G}$, which is evident from Fig. 3(a). We perform an extensive numerical search over a set of 10^7 three-qubit pure states from each of the W and the GHZ classes, and find that for all instances, $E_{GL} = E_L^{r'}$, when the bipartition r':rest provides $\mathcal{G}$ – an observation similar to what is found in the case of single-qubit measurement on an N-qubit gW state. When $r \neq r'$, $E_L^r = \mathcal{G}$. These findings lead us to the following conjecture:

- *If the maximal Schmidt coefficient for an arbitrary three-qubit pure state is obtained across the bipartition r:rest, $r \in \{1, 2, 3\}$, then $E_{GL} = E_L^{r'} \geq \mathcal{G}$ with $r' \in \{1, 2, 3\}$ when $r' = r$. On the other hand, $E_L^{r'}$ coincides with $\mathcal{G}$ when $r' \neq r$.*

This conjecture helps to pin-point the position of measurement while one tries to increase the value of genuine multiparty entanglement by means of localization.

To investigate arbitrary four-qubit pure states, we focus on the classes given by $|\Psi_i^4\rangle$, $i = 1, 2, \cdots, 6$, from the nine parametric classes of four-qubit states [49, 50] (see Appendix F). Note that in all instances except $|\Psi_6^4\rangle$, the LGGM is found to be upper bounded by the GGM of the original state (see Fig. 3(b)), when measurement is performed on qubit 1. This result remains unchanged with a change in the position of the measured qubit, as indicated by Fig. 3(c), where results corresponding to measurement over qubit 2 in the cases of $|\Psi_3^4\rangle$, $|\Psi_5^4\rangle$, and $|\Psi_6^4\rangle$ are presented. The LGGM of the states $|\Psi_i^4\rangle$, $i = 7, 8, 9$, with single-qubit measurement, can be obtained analytically, and are tabulated in Table II.

In the case of Haar-uniformly generated arbitrary four-qubit pure states, about 29% of states are found to have $E_L^1 > \mathcal{G}$, as depicted in Fig. 3(d). Interestingly, when local measurements over qubits 1 and 2 are performed, about 22% of the 71% states for which $\mathcal{G} > E_L^1$ are found to have $E_L^{\{1,2\}} > \mathcal{G}$. Also, for about 47.6% of such states, $E_L^{\{1,2\}} > E_L^1$. Qualitatively similar results are found when random four-qubit states are sampled Haar-uniformly from the parametrized four-qubit classes [49, 50]. For example, the LGGM of about 20.4% of the four-qubit states of the form $|\Psi_1^4\rangle$, for which $E_L^1 \leq \mathcal{G}$, can be increased beyond the value of $\mathcal{G}$, when local measurements over qubits 1 and 2 are performed (Fig. 3(e)). Moreover, for about 44.9% of the states, $E_L^{\{1,2\}} > E_L^1$. Hence, the results again indicate that local measurements on two parties can be more advantageous than the measurement on a single party for some multiparty states. The values of $E_L^{\{r_1,r_2\}}$, where $r_1 \neq r_2$ with $r_{1,2} \in \{1, 2, 3, 4\}$, in the case of the states $|\Psi_i^4\rangle$, $i = 7, 8, 9$, are tabulated in Table II. Note that the state $|\Psi_7^4\rangle$, provides an example of a four-qubit pure state for which $E_L^{\mathbf{r}_\alpha} = \mathcal{G}\ \forall\ \mathbf{r}_\alpha$, where $\alpha = 1, 2, \cdots, \binom{N}{m}$, $m = 1, 2$. Note also that $|\Psi_8^4\rangle$ presents an example of a four-qubit state for which a $E_L^r > \mathcal{G}$ only when measurement is performed over a specific qubit, and measurement over two qubits can enhance the value of LGGM over the single-qubit measurement.

It is evident from Figs. 3(b)-(e) that the arbitrary four-qubit pure states as well as four-qubit pure states of the form $|\Psi_i^4\rangle$, $i = 1, \ldots, 6$, are not uniformly distributed over the $\mathcal{G} - E_L^r$ and $\mathcal{G} - E_L^{\{r_1,r_2\}}$ planes, $r, r_1, r_2 = 1, \ldots, 4$, but cluster around specific regions. In the case of E_L^1, one of the boundaries of the accessible region is always the line $E_L^1 = \mathcal{G}$ when $|\Psi_i^4\rangle$, $i = 1, \ldots, 4$ are considered. For $|\Psi_5^4\rangle$ and $|\Psi_6^4\rangle$, the situation is different, and all the states lie on very restricted regions on the $\mathcal{G} - E_L^r$ plane. Such clustering is found in the case of five-qubit arbitrary pure states also, which highlights the importance of finding the quantum states that lies in a beneficial region, i.e.,

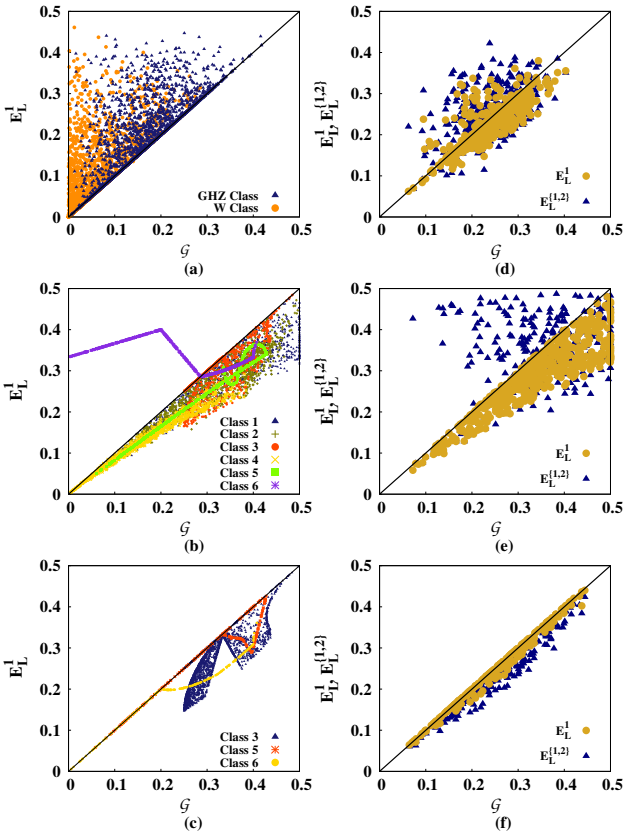

FIG. 3. (Color online.) Scatter plots. **(a)** E_L^1 vs. $\mathcal{G}$ for three-qubit pure states belonging to the GHZ class and the W class. **(b)** E_L^1 vs. $\mathcal{G}$ for the four-qubit classes represented by $|\Psi_i^4\rangle$, $i = 1, \cdots, 6$. **(c)** E_L^2 vs. $\mathcal{G}$ for the four-qubit classes represented by $|\Psi_i^4\rangle$, $i = 3, 5, 6$. **(d)** E_L^1 and $E_L^{\{1,2\}}$ vs. $\mathcal{G}$ in the case of arbitrary four-qubit pure states. **(e)** E_L^1 and $E_L^{\{1,2\}}$ vs. $\mathcal{G}$ for four-qubit states of the form $|\Psi_1^4\rangle$. and **(f)** E_L^1 and $E_L^{\{1,2\}}$ vs. $\mathcal{G}$ for four-qubit symmetric states of the form $|D_g^N\rangle$. Each plot constitutes of 10^5 Haar-uniformly generated pure states. All quantities plotted are dimensionless.

where $E_L^r \geq \mathcal{G}$, or $E_L^{\{r_1,r_2\}} \geq \mathcal{G}$. However, Haar-uniform numerical simulation of arbitrary pure states becomes difficult as the number of qubits increases, thereby restricting the investigation of the behavior of LGGM against the GGM of the original state in the case of $N > 5$.

We conclude by mentioning that similar to the case of single-qubit measurement, in the case of $|D_g^N\rangle$ (Eq. (10)), $E_L^{\{r_1,r_2\}} \leq \mathcal{G}$, where $r_1 \neq r_2$, and $r_{1,2} \in \{1, 2, \cdots, N\}$. Note here that the symmetry present in the states $|D_g^N\rangle$ guarantees that all pairs of qubits chosen for local measurement are equivalent. Also, in contrast to the previous examples of two-qubit measurements, in this case, an increase in m is found to result, for an overwhelmingly large fraction of states, in a decrease in the value of LGGM. For example, in about 99.1% of $|D_g^4\rangle$, $E_L^{\{r_1,r_2\}} < E_L^1$, while for $N = 5$, the fraction is 93.9%. The variation of LGGM against GGM for $|D_g^4\rangle$ is depicted in Fig. 3(f).

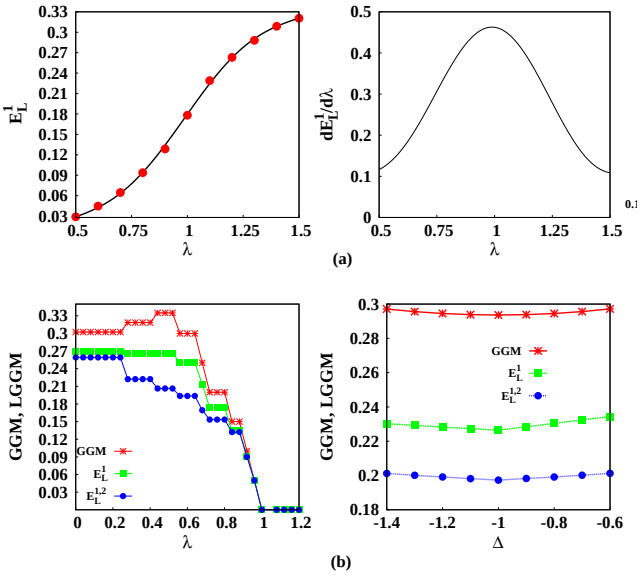

FIG. 4. (Color online.) **(a)** Variations of E_L^1 (left panel), and $dE_L^1/d\lambda$ (right panel) as functions of $\lambda = J/h$ for the transverse-field Ising model with $N = 16$. **(b)** Variation of $\mathcal{G}$, E_L^1, and $E_L^{\{1,2\}}$ as functions of λ with $\Delta = 0.5$ (left panel) and Δ with $\lambda = 0$ (right panel) for $N = 20$. All quantities plotted are dimensionless.

IV. LGGM IN QUANTUM SPIN MODELS

For the past fifteen years or so, probing interesting physical phenomena observed in many-body systems using quantum information theoretic tools and techniques has been an active cross-disciplinary field of research [9, 10, 12–14, 51–53]. Realization of quantum spin Hamiltonians in various substrates, such as solid state systems [54], optical lattice [20, 55, 56], ion traps [12, 57], and NMR [58] under controlled laboratory environments have allowed researchers to test the properties of several information theoretic measures of quantum correlations in well-known quantum spin models. In this section, we discuss the behavior of LGGM in the vicinity of quantum phase transitions (QPT) [42], when the pure state, for which LGGM is calculated, is the ground state of well-known 1d quantum spin models.

It is interesting to mention here that a similar set of results was obtained in Ref. [36] by using the concept of localizable entanglement. An important difference of the results there with those in this paper is that the plots and the corresponding analyses here are directly for the LGGM, while those in Ref. [36] are often for bounds on localizable entanglement. In this context, we would like to set emphasis on the fact that the computation of LGGM in a multiqubit state with high number of qubits can also be involved. On one hand, one has to perform an optimization over $2m$ real parameters (see discussion in Sec. III A) with m being the number of measured qubits. On the other hand, in order to calculate LGGM corresponding to local measurement over m qubits in an N-qubit pure state, GGM of $(N - m)$-partite pure states in the post-measurement ensemble needs to be computed. Typically, for an $\tilde{N}$-qubit pure state, computation of GGM in its full generality requires consideration of the maxi-

mum eigenvalues of a total of $\sum_{i=1}^{\tilde{N}/2}\binom{\tilde{N}}{i}$ density matrices of dimensions 2^i, $i = 1, \ldots, \tilde{N}/2$, indicating an exponential increase of the computational complexity of LGGM with increasing $\tilde{N}$. Also, exact computation of LGGM for the ground state of a spin Hamiltonian constituted of N spins requires access to the exact ground state of the Hamiltonian, the determination of which is non-trivial for high values of N. Therefore, we use Lanczos diagonalization technique [59] to determine the ground states of the spin Hamiltonians when N is large, and use the symmetries of the ground state to reduce the computational complexity.

A. Transverse-field Ising Model

The first model we discuss is the transverse-field quantum Ising model [43] in 1d, with periodic boundary condition (PBC), whose Hamiltonian is given by

$$H = J\sum_{i=1}^{N}\sigma_i^x\sigma_{i+1}^x + h\sum_{i=1}^{N}\sigma_i^z. \tag{11}$$

Here, J and h respectively are strengths of the nearest-neighbor exchange coupling and the external magnetic field, $\sigma_i^{x,z}$ are the Pauli spin matrices, and N is the number of qubits in the system. Under PBC, $\sigma_{N+1} \equiv \sigma_1$. Both J and h are chosen to be positive. The model is known to undergo a QPT at the critical value of the parameter $\lambda = \lambda_c \equiv 1$ [13, 14, 42, 43, 51, 52], where $\lambda = J/h$, from an anti-ferromagnetic ($J > h$) to a paramagnetic phase ($J < h$). A few studies of the behavior of multipartite entanglement measures across QPT in quantum spin models are available [9, 10, 53] due to the difficulty of computing such measures. However, the investigation of bipartite measures has extensively been carried out [12, 13].

To overcome the difficulty in computing LGGM for higher number of parties, we first look into systems comprised of a relatively smaller number of parties (say as $N = 8, 10, 12$), and compute the LGGM of the ground state without any approximation. We find that irrespective of the value of N, in the case of single-qubit measurement, the maximization involved in Eq. (6) can be achieved by using the computational basis $\{|0\rangle, |1\rangle\}$ (see also [60]). Moreover, in the case of single-qubit measurement, the GGM of the $(N-1)$-qubit pure states in the post-measurement ensemble is always obtained from either the 1:rest, or the 2:rest bipartitions. We use these information to compute the LGGM for the ground state of the system with high values of N. Note that the 1d transverse-field Ising model can be solved by successive application of the Jordan-Wigner and Bogoliubov transformations [43]. However, this does not provide access to an analytical form of the ground state, from which LGGM can be computed. We determine the ground state of the model with high values of N via the Lanczos diagonalization scheme, and investigate the behavior of LGGM close to the QPT point. Fig. 4(a) (left panel) depicts the variation of E_L^1 against λ in the ground state of the model with $N = 16$. The points in the graph represents the numerical values of E_L^1 obtained by using the approximations discussed above, while the continuous line represents the fitted curve. The first derivative of E_L^1 with λ, as obtained from the fitted curve, shows a maximum at the QPT point $\lambda_c = 1$ (Fig. 4(a), right panel). The maximum sharpens with increasing N.

B. XXZ model in an external field

The Hamiltonian describing the 1d XXZ model [44–47], under PBC, is given by

$$H' = J'\sum_{i=1}^{N}(\sigma_i^x\sigma_{i+1}^x + \sigma_i^y\sigma_{i+1}^y - \Delta\sigma_i^z\sigma_{i+1}^z) + h'\sum_{i=1}^{N}\sigma_i^z, \tag{12}$$

where J' and h' represent respectively the nearest-neighbor exchange coupling and the external field-strength, while Δ is the (dimensionless) anisotropy in the z direction. Although the model can be solved using the thermodynamic Bethe ansatz technique [44, 47], an analytical form of the LGGM or any multipartite entanglement measure is still elusive due to the inaccessibility of the analytical form of the exact ground state. Similar to the case of the transverse Ising model, we probe the phase diagram [47] of this model using LGGM as the physical quantity, where the ground state is obtained via Lanczos diagonalization method for different values of the system parameters, Δ and h'/J'. The observations in the transverse-field Ising model, such as obtaining the GGM of the post-measurement pure states from either the 1:rest, or the 2:rest bipartitions, in the case of smaller number of spins, are found to be valid here even for local measurement over two qubits. An assumption of the validity of these observations in the case of large N, considerably reduces the complexity of computation. Fig. 4(b) (left panel) shows the variations of $\mathcal{G}$, E_L^1, and $E_L^{\{1,2\}}$ against $\lambda \equiv h'/J'$ for the ground state of the Hamiltonian given in Eq. (12), with $N = 20$ and $\Delta = 0.5$. With increasing λ, all the quantum correlation measures become zero at $\lambda = \lambda_c \equiv 1$, signaling a transition of the ground state from an entangled to a product state [45, 47]. The z-component of the total spin is a conserved quantity of the system due to the presence of $\mathbb{Z}_2$ symmetry in the Hamiltonian, thereby making the Hamiltonian block-diagonalizable. The plateaus in the variations of GGM and LGGM with λ correspond to different values of the z-component of the total spin. With increasing N, the number of the plateaus increases, while the widths of the individual plateaus decrease, and the curves eventually tend to continuous ones for high values of N.

In the absence of the external magnetic field, the ground state of the model experiences a KT transition [45] at $\Delta = -1$, which is signaled by a blunt minimum in the $\mathcal{G}$ vs. Δ curve (see Fig. 4(b) (right panel)). On the other hand, the LGGMs, namely E_L^1 and $E_L^{\{1,2\}}$, show a sharper cusp at $\Delta = -1$, correctly signaling the KT transition. Therefore, similar to localizable entanglement [36], LGGM also signals the KT transition, which is usually not detected by the frequently-used quantum information theoretic quantities in detecting QPTs [61].

Note here that even for a small system where finite-size effects are expected to play a considerable role, LGGM serves as a satisfactory indicator of quantum critical phenomena. Hence, LGGM is expected to find its applicability in the investigation of quantum cooperative phenomena observed in many-body systems beyond the quantum spin models.

V. CONCLUDING REMARKS

Multipartite entanglement has been proven to be useful for the successful implementation of several quantum information theoretic protocols. In the present paper, we consider the conceptualization and use of localizable multipartite entanglement, obtained by performing a local measurement at a few parties. The notion of localizable multiparty entanglement depends on the understanding and computability of another measure of multiparty entanglement of a lower number of parties, which we refer to as the seed measure. We use the geometric measure in general, and the generalized geometric measure in particular, as the see measure. In the case when the seed measure is the generalized geometric measure, the localizable multiparty entanglement measure is called the localizable generalized geometric measure. We discuss its various properties, and in particular, we analytically consider the behavior of the measure for a number of paradigmatic examples of multipartite pure states, where the localization is achieved via local rank-1 projective measurement over a single qubit. The examples include the N-qubit generalized GHZ and W states, Dicke states, and the generalized superposition of Dicke states for fixed number of qubits. We show that for the N-qubit generalized GHZ and W states, the localization of generalized geometric measure by local projection measurement over one qubit always results in a value of localizable multipartite entanglement which is greater than, or equal to the multipartite entanglement present in the original state. Our numerical simulations seem to indicate that such enhancement due to measurement holds for arbitrary three-qubit pure states. However, for higher number of parties, no such lower bound exists. We also show that for the N-qubit Dicke states, the localizable multipartite entanglement achieved via single-qubit measurement is bounded above by the generalized geometric measure of the original state.

To investigate whether measurement over more than one qubit helps in achieving a better localization of multipartite entanglement than a single-qubit measurement, we consider several examples of multi-qubit pure states. We show that there exists multiqubit states in which local measurement over two qubits yields higher values of localizable generalized geometric measure compared to single-qubit measurement. However, this phenomenon is not generic for arbitrary multiqubit states, as shown from our numerical simulations. We finally inquire whether there exists a situation in which LGGM is more powerful than its parent multipartite entanglement measure, the GGM. We show that this is indeed the case for detecting QPT in the many-body systems. Specifically, we show that the derivatives of LGGM can signal QPT of the transverse-field Ising model more accurately even for a smaller system-size, achievable in current experiments, compared to that of the GGM. We also show that LGGM detects the KT transition of the XXZ model better than its parent multiparty measure.

Appendix A: Multipartite entanglement measures

The geometric measure of entanglement of an N-partite state $|\tilde{\Psi}_N\rangle$, is defined as

$$G_K(|\tilde{\Psi}_N\rangle) = 1 - \max_{\mathcal{S}_K} |\langle\tilde{\Phi}_N^K|\tilde{\Psi}_N\rangle|^2, \tag{A1}$$

where K ($2 \leq K \leq N$) is an integer denoting the number of product state partitions into which the N-partite state $|\tilde{\Phi}_N^K\rangle$ can be divided [1, 9, 10, 25–28]. The distance of the state $|\tilde{\Psi}_N\rangle$ is minimized over the set, $\mathcal{S}_K$, of all K-separable pure states, $|\tilde{\Phi}_N^K\rangle$, and we refer to this measure as K-GM. For example, $K = N$ corresponds to a fully separable state $|\tilde{\Phi}_N^N\rangle \equiv \bigotimes_{i=1}^N |\tilde{\phi}_i\rangle$, leading to the original definition of GM [25, 28]. On the other hand, GGM is obtained for $K = 2$ [10, 27], the other extremum of K-GM, which we denote by $\mathcal{G}(|\tilde{\Psi}_N\rangle)$. The optimization in the definition of $\mathcal{G}(|\tilde{\Psi}_N\rangle)$ can be performed by using the maximization of the Schmidt coefficients across all possible bipartitions of $|\tilde{\Psi}_N\rangle$, leading to the simplified version of GGM [10], given by

$$\mathcal{G}(|\tilde{\psi}_N\rangle) = 1 - \max_{\mathcal{S}_{\mathcal{A}:\mathcal{B}}} \{\lambda^2_{\mathcal{A}:\mathcal{B}}\}. \tag{A2}$$

Here, $\lambda_{\mathcal{A}:\mathcal{B}}$ is the maximum Schmidt coefficient of $|\tilde{\Psi}_N\rangle$, the maximum being taken over the set, $\mathcal{S}_{\mathcal{A}:\mathcal{B}}$, of all arbitrary $\mathcal{A} : \mathcal{B}$ bipartitions such that $\mathcal{A} \cup \mathcal{B} = \{1, 2, \cdots, N\}$, and $\mathcal{A} \cap \mathcal{B} = \mathbf{\Phi}$, the null set. The above expression allows one to compute GGM of a multiparty pure state in arbitrary dimensions and for arbitrary number of parties.

Appendix B: Proofs of the Propositions

Proposition I. Once the rank-1 projective measurement is performed over the first qubit, an ensemble of two pure states, $\{p^l, |\Psi^l\rangle\}$, $l = 1, 2$, is obtained, where $p^l = |a_1|^2 q_1^l + |a_2|^2 q_2^l$, $|\Psi^l\rangle = |\xi_1^l\rangle \otimes |\psi^l\rangle$ for $l = 1, 2$, and $|\psi^l\rangle = (a_1 z_1^l |0\rangle^{\otimes N-1} + a_2 z_2^l |1\rangle^{\otimes N-1})/\sqrt{p^l}$. The quantities $q_{1,2}^l$ and $z_{1,2}^l$ are given by

$$\begin{aligned} q_1^l &= (\delta_{1l} c^2_{\theta/2} + \delta_{2l} s^2_{\theta/2}), \\ q_2^l &= (\delta_{1l} s^2_{\theta/2} + \delta_{2l} c^2_{\theta/2}), \end{aligned} \tag{B1}$$

and

$$\begin{aligned} z_1^l &= \delta_{1l} c_{\theta/2} - \delta_{2l} e^{-i\phi} s_{\theta/2}, \\ z_2^l &= \delta_{1l} e^{i\phi} s_{\theta/2} + \delta_{2l} c_{\theta/2}, \end{aligned} \tag{B2}$$

with δ_{kl}, $k = 1, 2$, being Kronecker delta. Note that the states $|\psi^l\rangle$ are of the form of an $(N-1)$-qubit gGHZ state. Note also that for an N-qubit gGHZ state, the local density matrix, ρ_n, of n qubits, is diagonal in the computational basis with only two non-zero elements. Hence, in the present case, the LGGM of the gGHZ state can be obtained from Eq. (6), where $\mathcal{G}(\psi^l_{N-1}) = 1 - \max\left\{|a_1|^2 q_1^l/p^l, |a_2|^2 q_2^l/p^l\right\}$ with $p^l = |a_1|^2 q_1^l + |a_2|^2 q_2^l$. Using the identity, $\max\{x, y\} + \max\{u, v\} = \max\{x+u, x+v, y+u, y+v\}$ for arbitrary values of x, y, u, and v, in Eq. (6), one obtains

$$E_L^1 = 1 - \min_\theta \left[\max\left\{|a_1|^2, s^2_{\theta/2}, c^2_{\theta/2}\right\}\right]. \tag{B3}$$

In $[0,\pi]$, $c^2_{\theta/2}$ is a monotonically decreasing function whereas $s^2_{\theta/2}$ is a monotonically increasing one, and the maximum value of both the functions is unity, occurring at $\theta = 0$ for $c^2_{\theta/2}$, and $\theta = \pi$ for $s^2_{\theta/2}$. Besides, the values of both functions are equal to $1/2$ at $\theta = \pi/2$. Since $|a_1|^2 \geq 1/2 \geq |a_2|^2$, the allowed range of θ can be divided into three subregions: **(i)** $0 \leq \theta \leq \theta_1$, where $c^2_{\theta/2} \geq |a_1|^2 \geq s^2_{\theta/2}$, **(ii)** $\theta_1 < \theta < \theta_2$, where $|a_1|^2 \geq \max\{c^2_{\theta/2}, s^2_{\theta/2}\}$, and **(iii)** $\theta_2 \leq \theta \leq \pi$, where $s^2_{\theta/2} \geq |a_1|^2 \geq c^2_{\theta/2}$. Here, the values of θ_1 and θ_2 are obtained as solutions of the equations $c^2_{\theta/2} = |a_1|^2$ and $s^2_{\theta/2} = |a_1|^2$ respectively. The maximization inside the curly bracket in Eq. (B3) has to be performed for a fixed value of θ, which can be chosen from any one of the three subregions, **(i)**, **(ii)**, and **(iii)**. Noticing that $\min(c^2_{\theta/2}) = |a_1|^2$ for $0 \leq \theta \leq \theta_1$, while $\min(s^2_{\theta/2}) = |a_1|^2$ in the region $\theta_2 \leq \theta \leq \pi$, from Eq. (B3), one obtains $E^1_L = |a_2|^2$. Note here that the GGM of the gGHZ state, under the assumption that $|a_1|^2 \geq \frac{1}{2} \geq |a_2|^2$, is also $|a_2|^2$, leading to $E^1_L = \mathcal{G}$. ■

Proposition II. The post measurement ensemble is $\{p^l = (|a_2|^2 + |a_3|^2)q^l_1 + |a_1|^2 q^l_2, |\psi^l\rangle = [z^l_1(a_2|10\rangle + a_3|01\rangle) + z^l_2 a_1|00\rangle]/\sqrt{p^l}\}$, $l = 1, 2$, where $z^l_{1,2}$ and $q^l_{1,2}$ are given in Eqs. (B1) and (B2) respectively. One must note that the GGM of two-qubit states of the form $|\psi^l\rangle$ is invariant under an interchange of a_2 and a_3. The LGGM (Eq. (6)), in this case, is given by

$$E^1_L = \frac{1}{2}\left(1 - \min_\theta \sum_{l=1}^{2} \sqrt{f^l(\theta)}\right), \tag{B4}$$

where $f^l(\theta) = p^{l\,2} - 4|a_2|^2|a_3|^2 u^l$, and

$$u^l = \delta_{1l} c^4_{\theta/2} + \delta_{2l} s^4_{\theta/2}. \tag{B5}$$

The validity of the single qubit density matrix ρ^l_2 of qubit 2, obtained from the state $|\psi^l\rangle$, demands that $f^l(\theta) \geq 0\ \forall\ \theta$. The function $f(\theta) = \sum_{l=1}^{2} \sqrt{f^l(\theta)}$ has minimum at $\theta = 0, \pi$ in the interval $0 < \theta < \pi$, while having a maximum at $\theta = \pi/2$. Hence the optimization in LGGM, in this case, is achieved when measurement is performed in the $\{|0\rangle, |1\rangle\}$ basis. From Eq. (B4), it can be shown that $E^1_L = \min\{|a_2|^2, |a_3|^2\}$. In general, for the local projective measurement being performed on the qubit r, $E^r_L = \min\{|a_j|^2, |a_k|^2\}$, where $r \neq j \neq k$, and $r, j, k \in \{1, 2, 3\}$. This leads us to a non-trivial lower bound of LGGM for the tripartite gW state, which is invariant to a change in the choice of the measured qubit, as given by the following proposition.

We first consider $r = 1$. Let us first assume $|a_1|^2 \geq |a_2|^2 \geq |a_3|^2$, which leads to $\mathcal{G} = \min\{|a_j|^2\}$, $j = 2, 3$. Assuming other orderings and considering all the cases, we obtain $\mathcal{G} = \min\{|a_i|^2\}$, $i = 1, 2, 3$. If $|a_i|^2 \in \{|a_2|^2, |a_3|^2\}$, then $E^1_L = \mathcal{G}$. Else, $\mathcal{G} = |a_1|^2$, implying $E^1_L = \min\{|a_2|^2, |a_3|^2\} \geq \mathcal{G}$. Similar proofs hold when $r = 2, 3$. ■

Proposition III. As in the case of three-qubit systems, here also we start from the case $r = 1$. The GGM of the state $|W_N\rangle_g$ can be obtained as $\mathcal{G} = 1 - \max\{\lambda^{max}_n\}$, where λ^{max}_n is the maximum eigenvalue of all possible n-qubit reduced density matrices, $\rho^{\mathbf{s}}_n$, where $1 \leq n \leq N/2$ ($1 \leq n \leq (N-1)/2$) for even (odd) N. Here, "$\mathbf{s}$" denotes the set of all possible indices $\{s_j\}$, $j = 1, \cdots, n$, that represents the positions of the n qubits with $s_j \in \{1, 2, \cdots, N\}$. The density matrices, $\rho^{\mathbf{s}}_n$, can be written as

$$\rho^{\mathbf{s}}_n = P\left[\sum_{j=1}^{n} a_{s_j}|0\rangle^{\otimes(j-1)}|1\rangle_j|0\rangle^{\otimes(N-j)}\right] + \sum_{\substack{k=1 \\ k\notin\mathbf{s}}}^{N} |a_k|^2 P[|0\rangle^{\otimes n}], \tag{B6}$$

where $P[|a\rangle] = |a\rangle\langle a|$. From Eq. (B6), it is clear that the maximal eigenvalue is obtained from the case $n = 1$, and from the single qubit density matrix for which $|a_{s_1}|^2 = \min\{|a_i|^2\}$, $i = 1, 2, \cdots, N$, leading to $\mathcal{G} = |a_{s_1}|^2$.

To determine the LGGM, we first consider a measurement in the computational basis, $\{|0\rangle, |1\rangle\}$. A measurement over the first qubit in this basis leads to a product state, $|0\rangle^{\otimes(N-1)}$, with probability $p_0 = |a_1|^2$, and a pure state $|\Phi^{N-1}\rangle$, with probability $\sum_{i=2}^{N} |a_i|^2$, which can be identified as an $(N-1)$-qubit gW state. From the above discussion, $\mathcal{G}(|\Phi^{N-1}\rangle) = |a_j|^2/\sum_{i=2}^{N}|a_i|^2$, where $|a_j|^2 = \min\{|a_i|^2\}$, $i = 2, 3, \cdots, N$. The definition of LGGM implies $E^1_{L,0} = |a_j|^2$, where the subscript "0" indicates that the measurement is performed in the basis $\{|0\rangle, |1\rangle\}$. Clearly, $|a_j|^2 \geq |a_{s_1}|^2 \equiv \mathcal{G}$. Since the definition of LGGM involves a maximization over the complete set of projective measurements, $E^1_L \geq E^1_{L,0} \geq \mathcal{G}$. Similarly, one can prove for the cases $r = 2, 3, \cdots, N$, and hence the proof. ■

Proposition IV. Let us consider a gW state with the ordering $|a_1|^2 \leq |a_2|^2 \leq \cdots \leq |a_N|^2$. Assuming local projective measurement in qubit 1, $\mathcal{G} = |a_1|^2$ and $E^1_L = |a_2|^2$. The assumed ordering suggests that $\max\{|a_2|^2\} = (1 - |a_1|^2)/(N-1)$, which corresponds to the LGGM of a gW state of the form $|\Phi\rangle = |a_1||1\rangle|0\rangle^{\otimes N-1} + \sum_{j=2}^{N} a_j|0\rangle^{\otimes(j-1)}|1\rangle_j|0\rangle^{\otimes(N-j)}$, with $\mathcal{G} = |a_1|^2$, similar to the arbitrary gW state, and $|a_j|^2 = (1 - |a_1|^2)/(N-1)$, $j = 2, 3, \cdots, N$. Since $\mathcal{G} = |a_i|^2 = \min\{|a_k|^2\}$ for an arbitrary N-qubit gW state with arbitrary ordering of $\{|a_k|^2\}$, $k = 1, 2, \cdots, N$, one can prove similar result for each possible ordering of $\{|a_k|^2\}$, when measurement over qubit 1 is assumed. The result also holds for an arbitrary position, r, of the measured qubit, when $r \in \{1, 2, \cdots, N\}$. Hence the proof. ■

Appendix C: Single-qubit measurement on symmetric states

Since Dicke states are symmetric, the value of LGGM is independent of the position of the qubit over which measurement is performed, and the post measurement ensemble, $\{p^l, \psi^l\}$, is given by $p^l = A_k q^l_1 + B_k q^l_2$ and $|\psi^l\rangle = \sqrt{A_k} z^l_1 |D^{N-1}_k\rangle + \sqrt{B_k} z^l_2 |D^{N-1}_{k-1}\rangle$, with $A_k = \binom{N-1}{k}/\binom{N}{k}$, and $B_k = \binom{N-1}{k-1}/\binom{N}{k}$, while $q^l_{1,2}$ and $z^l_{1,2}$ being defined in Eqs. (B1) and (B2). To determine the LGGM of $|D^N_k\rangle$, one needs to calculate the GGM of $|\psi^l\rangle$, which, in turn, requires determination of the reduced density matrix of n qubits, $\rho^{l,\mathbf{s}}_n$, labeled with the set of indices $\mathbf{s} \equiv \{s_1, s_2, \cdots, s_n\}$. Since measurement over any single qubit of $|D^N_k\rangle$ yields an ensemble of symmetric states, the reduced density matrix, $\rho^{l,\mathbf{s}}_n$, of all possible collection of n

qubits of the state $|\psi^l\rangle$, are equivalent. Therefore, discarding the index "s", ρ_n^l can be obtained from $|\psi^l\rangle$ as

$$\rho_n^l = \frac{1}{\binom{N}{k}p^l}\Big[\sum_{i=0}^{n} F_i^l P[|D_i^n\rangle] - (-1)^l \sum_{i=0}^{n-1} G_i\Big(e^{-i\phi}|D_{i+1}^n\rangle\langle D_i^n| + e^{i\phi}|D_i^n\rangle\langle D_{i+1}^n|\Big)\Big], \tag{C1}$$

with $1 \le n \le N'$, where $N' = (N-2)/2$ ($N' = (N-1)/2$) when N is even (odd), and

$$F_i^l = \binom{n}{i}\left[\binom{N-n-i}{k-i}q_1^l + \binom{N-n-i}{k-i-1}q_2^l\right]$$
$$G_i = \frac{s_\theta}{2}\binom{N-n-1}{k-i-1}\sqrt{\binom{n}{i+1}\binom{n}{i}}. \tag{C2}$$

The GGM of $|\psi^l\rangle$ is given by $\mathcal{G}^l = 1 - \max\{\Lambda_n^l\}$, $n = 1, 2, \cdots, N'$, where Λ_n^l is the maximum eigenvalue of ρ_n^l.

Similarly, for an arbitrary state $|D_g^N\rangle$ of the form (10), rank-1 projective measurement over qubit r, $r = 1, 2, \cdots, N$, produces an ensemble of two $(N-1)$-qubit symmetric states represented by $\{p^l, |\bar{D}_g^{N-1}\rangle\}$, where $p^l = \sum_{k=1}^{N-1}\binom{N-1}{k}|\bar{z}_1^l a_k + \bar{z}_2^l a_{k+1}|^2$, $|\bar{D}_g^{N-1}\rangle = \frac{1}{\sqrt{p^l}}\sum_{k=1}^{N-1}(\bar{z}_1^l a_k + \bar{z}_2^l a_{k+1})|D_k^{N-1}\rangle$, with $\bar{z}_1^l = \delta_{1l}c_{\theta/2} - (-1)^l\delta_{2l}e^{i\phi}s_{\theta/2}$, and $\bar{z}_2^l = \delta_{1l}e^{-i\phi}s_{\theta/2} + \delta_{2l}c_{\theta/2}$.

Appendix D: LGGM with local measurement over more than one qubit

Here we present two more examples of multipartite pure states for which local measurement over more than one qubit may turn out to be beneficial regarding the value of LGGM.

Example 1. Consider the four-qubit state given by $|\Psi_4\rangle = a(|0000\rangle + |0011\rangle + |1100\rangle + |1111\rangle) + \sqrt{(1-4a^2)/6}(|0101\rangle + |1010\rangle + |0110\rangle + |1001\rangle + |1011\rangle + |0100\rangle)$, where $a \le 1/2$, a being a real number. Note that unlike the four-qubit state considered in Sec. III B, this state does not belong to the set of gW states. However, similar to the former case, here also, $E_L^{\{1,2\}} > E_L^1$ for a finite range of the allowed values of the state-parameter a.

Example 2. Consider the five-qubit state given by $|\Psi_5\rangle = a(|00000\rangle + |00111\rangle + |11000\rangle + |11111\rangle) + \sqrt{(1-4a^2)/4}(|01010\rangle + |10101\rangle + |00001\rangle + |10000\rangle)$. Here again a finite parameter range can be obtained in which $E_L^{\{1,2\}} > \mathcal{G}$, although $E_L^1 < \mathcal{G}$.

These examples highlight the importance of two-qubit measurement in the cases where single-qubit measurement is not enough to increase the multipartite entanglement possessed by the original state. The results of our investigation on the existence of arbitrary multiqubit pure states, in which two-qubit measurements may yield better results than single-qubit ones, are presented in Sec. III C. Intuitively, one can argue that if one increases the number of parties in which the measurement is performed, it helps to concentrate entanglement and hence to increase LGGM. Although the above examples support such intuition, counter-examples also exist.

Appendix E: GHZ and W class of states

The normalized three-qubit states of the W-class, up to LU, are given by [38]

$$|\Phi_w\rangle = \sqrt{a_1}|001\rangle + \sqrt{a_2}|010\rangle + \sqrt{a_3}|100\rangle + \sqrt{a_4}|000\rangle \tag{E1}$$

with $a_1, a_2, a_3 > 0$, and $a_4 = 1 - (a_1 + a_2 + a_3) \ge 0$. Simple algebra dictates that the GGM of $|\Phi_w\rangle$ is given by $\mathcal{G} = 1 - \max\{\lambda_i\}$, $i = 1, 2, 3$, where $\lambda_i = [1 + (1 - 4((a_j + a_k)a_i)^{1/2}]/2$, with $i, j, k \in \{1, 2, 3\}$, and no two among i, j, k being equal. Now, LGGM of $|\Phi_w\rangle$ for $r = 1$ can be obtained as $E_L^1 = [1 - \min_{\theta,\phi} f_{wc}(\theta, \phi)]/2$, where

$$f_{wc}(\theta, \phi) = \sum_{l=1}^{2}(p^{l^2} - 4a_1a_2u^l)^{1/2}, \tag{E2}$$

and $p^l = (a_1 + a_2 + a_4)q_1^l + a_3q_2^l - (-1)^l\sqrt{a_3a_4}s_\theta c_\phi$, with $q_{1,2}^l$ and u^l given in Eqs. (B1) and (B5), respectively. The optimization of the above function leads to two equations involving the real parameters θ and ϕ. One of them implies $\phi = 0, \pi$ independent of the value of θ, while the second equation, independent of ϕ, has to be solved numerically for θ. Numerical solution of the latter provides the values of θ, which, along with $\phi = 0, \pi$, makes the Jacobian of $f_{wc}(\theta, \phi)$ positive semidefinite.

The normalized three-qubit states of the GHZ class, up to LU, can be represented by [38]

$$|\Phi_{ghz}\rangle = \sqrt{K}\left(c_\delta|000\rangle + e^{i\mu}s_\delta\bigotimes_{i=1}^{3}|\eta_i\rangle\right),$$

where $|\eta_i\rangle = c_{\gamma_i}|0\rangle + s_{\gamma_i}|1\rangle$, and $K^{-1} = 1 + 2c_\delta s_\delta c_{\gamma_1}c_{\gamma_2}c_{\gamma_3}c_\mu$, K being the normalization factor, and $K \in (1/2, \infty)$. The ranges for the five real parameters are $\delta \in (0, \pi/4]$, $\gamma_i \in (0, \pi/2]$, $i = 1, 2, 3$, and $\mu \in [0, 2\pi)$. Due to increased number of parameters, determination of GGM as well as LGGM for arbitrary GHZ class of states are to be achieved via numerical techniques.

Appendix F: Classes of four-qubit states

The nine classes of four-qubit states, as considered in [49, 50], are

$$|\Psi_1^4\rangle = \frac{1}{2}\{(a_1+a_2)(|0000\rangle+|1111\rangle)+(a_1-a_2)(|0011\rangle+|1100\rangle)+(a_3+a_4)(|0101\rangle+|1010\rangle)+(a_3-a_4)(|0110\rangle+|1001\rangle)\},$$
$$|\Psi_2^4\rangle = \frac{1}{2}\{(a_1+a_2)(|0000\rangle+|1111\rangle)+(a_1-a_2)(|0011\rangle+|1100\rangle)+2a_3(|0101\rangle+|1010\rangle+|0110\rangle),$$
$$|\Psi_3^4\rangle = a_1(|0000\rangle+|1111\rangle)+a_2(|0101\rangle+|1010\rangle+|0110\rangle+|0011\rangle),$$
$$|\Psi_4^4\rangle = \frac{1}{2}\{2a_1(|0000\rangle+|1111\rangle)+(a_1+a_2)(|0101\rangle+|1010\rangle)+(a_1-a_2)(|0110\rangle+|1001\rangle)+\sqrt{2}i(|0001\rangle+|0010\rangle+|0111\rangle+|1011\rangle)\},$$
$$|\Psi_5^4\rangle = a_1(|0000\rangle+|0101\rangle+|1010\rangle+|1111\rangle)+i|0001\rangle+|0110\rangle-i|1011\rangle,$$
$$|\Psi_6^4\rangle = a_1(|0000\rangle+|1111\rangle)+|0011\rangle+|0101\rangle+|0110\rangle,$$
$$|\Psi_7^4\rangle = |0000\rangle+|0101\rangle+|1000\rangle+|1110\rangle,$$
$$|\Psi_8^4\rangle = |0000\rangle+|1011\rangle+|1101\rangle+|1110\rangle,$$
$$|\Psi_9^4\rangle = |0000\rangle+|0111\rangle, \tag{F1}$$

where the complex parameters a_1, a_2, a_3, and a_4 have non-negative real parts.

[1] R. Horodecki, P. Horodecki, M. Horodecki, and K. Horodecki, Rev. Mod. Phys. **81**, 2 (2009).

[2] R. Raussendorf and H. J. Briegel, Phys. Rev. Lett. **86**, 5188 (2001); P. Walther, K. J. Resch, T. Rudolph, E. Schenck, H. Weinfurter, V. Vedral, M. Aspelmeyer, and A. Zeilinger, Nature **434**, 169 (2005); H. J. Briegel, D. Browne, W. Dür, R. Raussendorf, and M. van den Nest, Nat. Phys. **5**, 19 (2009).

[3] C. H. Bennet and S. J. Wiesner, Phys. Rev. Lett. **69**, 2881 (1992); K. Mattle, H. Weinfurter, P. G. Kwiat, and A. Zeilinger, Phys. Rev. Lett. **76**, 4656 (1996).

[4] D. Bruß, G. M. D'Ariano, M. Lewenstein, C. Macchiavello, A. Sen(De), and U. Sen, Phys. Rev. Lett. 93, 210501 (2004); D. Bruß, G. M. D'Ariano, M. Lewenstein, C. Macchiavello, A. Sen(De), and U. Sen, Int. J. Quant. Inf. **4**, 415-428 (2006).

[5] A. Sen(De) and U. Sen, Phys. News **40**, 17 (2010) (arXiv:1105.2412 [quant-ph]).

[6] A. Ekert, Phys. Rev. Lett. **67**, 661 (1991); T. Jennewein, C. Simon, G. Weihs, H. Weinfurter, and A. Zeilinger, Phys. Rev. Lett. **84**, 4729 (2000); D. S. Naik, C. G. Peterson, A. G. White, A. J. Berglund, and P. G. Kwiat, Phys. Rev. Lett. **84**, 4733 (2000); W. Tittel, T. Brendel, H. Zbinden, and N. Gisin, Phys. Rev. Lett. **84**, 4737 (2000); N. Gisin, G. Ribordy, W. Tittel, and H. Zbinden, Rev. Mod. Phys. **74**, 145 (2002).

[7] M. Żukowski, A. Zeilinger, M. A. Horne, and H. Weinfurter, Acta Phys. Pol. **93**, 187 (1998); M. Hillery, Vladimír Bužek, and André Berthiaume, Phys. Rev. A **59**, 1829 (1999); R. Demkowicz-Dobrzanski, A. Sen(De), U. Sen, and M. Lewenstein, Phys. Rev. A **80**, 012311 (2009).

[8] R. Cleve, D. Gottesman, and H.-K. Lo, Phys. Rev. Lett. **83**, 648 (1999); A. Karlsson, M. Koashi, and N. Imoto, Phys. Rev. A **59**, 162 (1999).

[9] T.-C. Wei, D. Das, S. Mukhopadyay, S. Vishveshwara, and P. M. Goldbart, Phys. Rev. A **71**, 060305(R) (2005); R. Orús, Phys. Rev. Lett. **100**, 130502 (2008); R. Orús, S. Dusuel, and J. Vidal, ibid. **101**, 025701 (2008); R. Orús, Phys. Rev. A **78**, 062332 (2008); Q.-Q. Shi, R. Orús, J. O. Fjærestad, and H.-Q. Zhou, New J. Phys. **12**, 025008 (2010). R. Orús and T.-C. Wei, Phys. Rev. B **82**, 155120 (2010); A. Sen(De) and U. Sen, arXiv:1002.1253 (2010); R. Prabhu, S. Pradhan, A. Sen(De), and U. Sen, Phys. Rev. A **84**, 042334 (2011); H. S. Dhar and A. Sen(De), J. Phys. A: Math. Theor. **44**, 465302 (2011); H. S. Dhar, A. Sen(De), and U. Sen, New J. Phys. **15**, 013043 (2013).

[10] A. Biswas, R. Prabhu, A. Sen(De), and U. Sen, Phys. Rev. A **90**, 032301 (2014).

[11] M. Sarovar, A. Ishizaki, G. R. Fleming, and K. B. Whaley, Nat. Phys. **6**, 462 (2010); J. Zhu, S. Kais, A. Aspuru-Guzik, S. Rodriques, B. Brock, and P. J. Love, J. Chem. Phys. **137**, 074112 (2012); N. Lambert, Y.-N. Chen, Y.-C. Cheng, C.-M. Li, G.-Y. Chen, and F. Nori, Nat. Phys. **9**, 10 (2013); T. Chanda, U. Mishra, A. Sen(De), and U. Sen, arXiv:1412.6519v2 [quant-ph] (2014), and references therein.

[12] M. Lewenstein, A. Sanpera, V. Ahufinger, B. Damski, A. Sen(De), and U. Sen, Adv. Phys. **56**, 243 (2007).

[13] L. Amico, R. Fazio, A. Osterloh, and V. Vedral, Rev. Mod. Phys. **80**, 517 (2008).

[14] K. Modi, A. Brodutch, H. Cable, T. Paterek, and V. Vedral, Rev. Mod. Phys. **84**, 1655 (2012).

[15] M.-F. Yang, Phys. Rev. A **71**, 030302 (2005); X.-F. Qian, T. Shi, Y. Li, Z. Song, and C.-P. Sun, Phys. Rev. A **72**, 012333 (2005); P. Lou and J.Y. Lee, Phys. Rev. B **74**, 134402 (2006); R. W. Chhajlany, P. Tomczak, A. Wójcik, and J. Richter, Phys. Rev. A **75**, 032340 (2007); D.I. Tsomokos, J.J. Garc a-Ripoll, N.R. Cooper, and J.K. Pachos, Phys. Rev. A **77**, 012106 (2008); C.-S. Yu, L. Zhou, and H.-S. Song, ibid. **77**, 022313 (2008); Z. Sun, X.-M. Lu, H.-N. Xiong, and J. Ma, New J. Phys. **11**, 113005 (2009); X. Peng, J. Zhang, J. Du, and D. Suter, Phys. Rev. A **81**, 042327 (2010); M. N. Bera, R. Prabhu, A. Sen(De), and U. Sen, arXiv:1209.1523 [quant-ph] (2012).

[16] D. Leibfried, E. Knill, S. Seidelin, J. Britton, R. B. Blakestad, J. Chiaverini, D. B. Hume, W. M. Itano1, J. D. Jost, C. Langer, R. Ozeri1, R. Reichle, and D. J. Wineland, Nature **438**, 639 (2005); T. Monz, P. Schindler, J. T. Barreiro, M. Chwalla, D. Nigg, W. A. Coish, M. Harlander, W. Hansel, M. Hennrich, and R. Blatt, Phys. Rev. Lett. **106**, 130506 (2011). J.T. Barreiro, J.-D. Bancal, P. Schindler, D. Nigg, M. Hennrich, T. Monz, N. Gisin and R. Blatt, Nat. Phys. **9**, 559 (2013), and references therein.

[17] R. Prevedel, G. Cronenberg, M. S. Tame, M. Paternostro, P. Walther, M. S. Kim, and A. Zeilinger, Phys. Rev. Lett. **103**, 020503 (2009); W.-B. Gao, C.-Y. Lu, X.-C. Yao, P. Xu, O. Gühne, A. Goebel, Y.-A. Chen, C.-Z. Peng, Z.-B. Chen, and J.-W. Pan, Nat. Phys. **6**, 331 (2010); Y.-F. Huang, B.-H. Liu, L. Peng, Y.-H. Li, L. Li, C.-F. Li, and G.-C. Guo, Nat. Comms. **2**, 546 (2011); X.-C. Yao, T.-X. Wang, P. Xu, H. Lu, G.-S. Pan, X-H. Bao, C.- Z. Peng, C.-Y. Lu, Y.-A. Chen, and J.-W. Pan, Nat. Photonics **6**, 225 (2012), and references therein.

[18] R. Barends, J. Kelly, A. Megrant, A. Veitia, D. Sank, E. Jeffrey,

T. C. White, J. Mutus, A. G. Fowler, B. Campbell, Y. Chen, Z. Chen, B. Chiaro, A. Dunsworth, C. Neill, P. OMalley, P. Roushan, A. Vainsencher, J. Wenner, A. N. Korotkov, A. N. Cleland, and J. M. Martinis, Nature **508**, 500 (2014), and references therein.

[19] C. Negrevergne, T.S. Mahesh, C.A. Ryan, M. Ditty, F. Cyr-Racine, W. Power, N. Boulant, T. Havel, D.G. Cory, and R. Laflamme, Phys. Rev. Lett. **96**, 170501 (2006), and references therein.

[20] O. Mandel, M. Greiner, A. Widera, T. Rom, T.W. Hänsch, and I. Bloch, Nature **425**, 937 (2003); I. Bloch, J. Phys. B: At. Mol. Opt. Phys. **38**, S629 (2005); P. Treutlein, T. Steinmetz, Y. Colombe, B. Lev, P. Hommelhoff, J. Reichel, M. Greiner, O. Mandel, A. Widera, T. Rom, I. Bloch, and T. W. Hänsch, Fortschr. Phys. **54**, 702 (2006); M. Cramer, A. Bernard, N. Fabbri, L. Fallani, C. Fort, S. Rosi, F. Caruso, M. Inguscio, and M.B. Plenio, Nat. Comm. **4**, 2161 (2013), and references therein.

[21] J. M. Raimond, M. Brune, and S. Haroche, Rev. Mod. Phys. **73**, 565 (2001); D. Leibfried, R. Blatt, C. Monroe, and D. Wineland, Rev. Mod. Phys. **75**, 281 (2003); K. Singer, U. Poschinger, M. Murphy, P. Ivanov, F. Ziesel, T. Calarco, F. Schmidt-Kaler, Rev. Mod. Phys. **82**, 2609 (2010); H. Haffner, C. F. Roose, R. Blatt, Phys. Rep. **469**, 155 (2008); L.-M. Duan, C. Monroe, Rev. Mod. Phys. **82**, 1209 (2010); J.-W. Pan, Z.-B. Chen, C.-Y. Lu, H. Weinfurter, A. Zeilinger, M. Żukowski, Rev. Mod. Phys. **84**, 777 (2012), and references therein.

[22] L. Henderson and V. Vedral, Phys. Rev. Lett. **84**, 2263 (2000); M. B. Plenio and V. Vedral, J. Phys. A: Math. Gen. **34**, 6997 (2001); V. Vedral, Rev. Mod. Phys. **74**, 197 (2002).

[23] D. A. Meyer and N. R. Wallach, J. Math. Phys. **43**, 4273 (2002).

[24] A. Osterloh and J. Siewert, Phys. Rev. A **72**, 012337 (2005); Int. J. Quant. Inf. **04**, 531 (2006); D. Ž. DJoković and A. Osterloh, J. Math. Phys. **50**, 033509 (2009); L. E. Buchholz, T. Moroder, O. Gühne, Ann. Phys. (Berlin) **528**, 278 (2016).

[25] A. Shimony, Ann. NY Acad. Sci. **755**, 675 (1995); H. Barnum and N. Linden, J. Phys. A **34**, 6787 (2001); T. -C. Wei, and P. M. Goldbart, Phys. Rev. A **68**, 042307 (2003); T. -C. Wei, M. Ericsson, P. M. Goldbart, and W. J. Munro, Quantum Inform. Compu. **4**, 252 (2004); D. Cavalcanti, Phys. Rev. A **73**, 044302 (2006),

[26] M. Blasone, F. Dell'Anno, S. DeSiena, and F. Illuminati, Phys. Rev. A **77**, 062304 (2008).

[27] A. Sen(De) and U. Sen, Phys. Rev. A **81**, 012308 (2010).

[28] J. Eisert and D. Gross, in Lectures on Quantum Information, edited by D. Bruss and G. Leuchs (Wiley-VCH, Weinheim, 2006).

[29] V. Coffman, J. Kundu, and W. K. Wootters, Phys. Rev. A **61**, 052306 (2000).

[30] R. Prabhu, A. K. Pati, A. Sen(De), and U. Sen, Phys. Rev. A **86**, 052337 (2012).

[31] A. Sen(De) and U. Sen, Phys. Rev. A **85**, 052103 (2012); M. N. Bera, R. Prabhu, A. Sen(De), and U. Sen, Phys. Rev. A **86**, 012319 (2012).

[32] D. M. Greenberger, M. A. Horne, and A. Zeilinger, in Bell's Theorem, Quantum Theory, and Conceptions of the Universe, ed. M. Kafatos (Kluwer Academic, Dordrecht, The Netherlands, 1989).

[33] D. P. DiVincenzo, C. A. Fuchs, H. Mabuchi, J. A. Smolin, A. Thapliyal, and A. Uhlmann, arXiv:quant-ph/9803033v1 (1998); T. Laustsen, F. Verstraete, and S. J. van Enk, Quantum Inf. Comput. **3**, 64 (2003); G. Gour, Phys. Rev. A **72**, 042318 (2005); J. A. Smolin, F. Verstraete, and A. Winter, Phys. Rev. A **72**, 052317 (2005); G. Gour, D. A. Meyer, and B. C. Sanders, Phys. Rev. A **72**, 042329 (2005); G. Gour, and R. W. Spekkens, Phys. Rev. A **73**, 062331 (2006); Z.-G. Li, S.-M. Fei, S. Albeverio, and W. M. Liu, Phys. Rev. A **80**, 034301 (2009).

[34] S. Popescu and D. Rohrlich, Phys. Lett. A **166**, 293 (1992).

[35] A. Sen(De), U. Sen, M. Wiesniak, D. Kaszlikowski, and M. Żukowski, Phys. Rev. A, **68**, 062306 (2003).

[36] F. Verstraete, M. Popp, and J. I. Cirac, Phys. Rev. Lett. **92**, 027901 (2004); M. Popp, F. Verstraete, M. A. Martín-Delgado, and J. I. Cirac, Phys. Rev. A **71**, 042306 (2005).

[37] A. Zeilinger, M. A. Horne, and D. M. Greenberger, in Proceedings of Squeezed States and Quantum Uncertainty, edited by D. Han, Y. S. Kim, and W. W. Zachary, NASA Conf. Publ. **3135**, 73 (1992).

[38] W. Dür, G. Vidal, J. I. Cirac, Phys. Rev. A **62**, 062314 (2000).

[39] R. Dicke, Phys. Rev. **93**, 99 (1954).

[40] G. Tóth, J. Opt. Soc. Am. B **24**, 275 (2007); S. Hartmann, arXiv:1201.1732 [quant-ph] (2012); M. Bergmann and O. Gühne, J. Phys. A: Math. Theor. **46**, 385304 (2013); B. Lücke, J. Peise, G. Vitagliano, J. Arlt, L. Santos, G. Tóth, and C. Klempt, Phys. Rev. Lett. **112**, 155304 (2014); A. Kumar, H. S. Dhar, R. Prabhu, A. Sen(De), and U. Sen, arXiv:1505.01748 [quant-ph] (2015).

[41] M. J. Holland and K. Burnett, Phys. Rev. Lett. **71**, 1355 (1993); R. Krischek, C. Schwemmer, W. Wieczorek, H. Weinfurter, P. Hyllus, L. Pezzé, and A. Smerzi, Phys. Rev. Lett. **107**, 080504 (2011); G. Tóth, Phys. Rev. A **85**, 022322 (2012); P. Hyllus, W. Laskowski, R. Krischek, C. Schwemmer, W. Wieczorek, H. Weinfurter, L. Pezz, and A. Smerzi, Phys. Rev. A **85**, 022321 (2012); A. Chiuri, C. Greganti, M. Paternostro, G. Vallone, and P. Mataloni, Phys. Rev. Lett. **109**, 173604 (2012); A. Noguchi, K. Toyoda, and S. Urabe, Phys. Rev. Lett. **109**, 260502 (2012).

[42] B. K. Chakrabarti, A. Dutta, and P. Sen, Quantum Ising Phases and Transitions in Transverse Ising Models (Springer, Heidelberg, 1996); S. Sachdev, Quantum Phase Transitions (Cambridge University Press, Cambridge, 2011); S. Suzuki, J. -I. Inou, B. K. Chakrabarti, Quantum Ising Phases and Transitions in Transverse Ising Models (Springer, Heidelberg, 2013).

[43] E. Lieb, T. Schultz, and D. Mattis, Ann. Phys. **16**, 407 (1961); E. Barouch, B. M. McCoy, and M. Dresden, Phys. Rev. A **2**, 1075 (1970); P. Pfeuty, Ann. Phys. **57**, 79 (1970); E. Barouch and B. M. McCoy, Phys. Rev. A **3**, 786 (1971).

[44] H. A. Bethe, Z. Phys. **71**, 205 (1931).

[45] C. N. Yang and C. P. Yang, Phys. Rev. **150**, 321 (1966); C. N. Yang and C. P. Yang, Phys. Rev. **150**, 327 (1966); A. Langari, Phys. Rev. B **58**, 14467 (1998); D. V. Dmitriev, V. Y. Krivnov, A. A. Ovchinnikov, and A. Langari, J. Exp. Theor. Phys. **95**, 538 (2002); S Mahdavifar, J. Phys.: Condens. Matter **19** 406222 (2007).

[46] H.-J. Mikeska, A. K. Kolezhuk, Lecture Notes in Physics **645**, 1 (2004).

[47] M. Takahashi, Thermodynamics of One-Dimensional Solvable Models (Cambridge University Press, Cambridge, 1999).

[48] W. K. Wootters, Phys. Rev. Lett. **80**, 2245 (1998); K. G. H. Vollbrecht and R. F. Werner, Phys. Rev. A **64**, 062307 (2001).

[49] F. Vestraete, J. Dehaene, B. De Moor, and H. Verschelde, Phys. Rev. A **65**, 052112 (2002).

[50] C. Eltschka and J. Siewert, J. Phys. A: Math. Theor. **47**, 424005 (2014).

[51] J. I. Latorre, and A. Rierra, J. Phys. A **42**, 504002 (2009); J. Eisert, M. Cramer, and M. B. Plenio, Rev. Mod. Phys. **82**, 277, (2010);

[52] A. Osterloh, L. Amico, G. Falci, and R. Fazio, Nature **416**, 608 (2002); T. Osborne, and M. Nielsen, Phys. Rev. A **66**, 032110 (2002); G. Vidal, J. Latorre, E. Rico, and A. Kitaev, Phys.Rev. Lett. **90**, 227902 (2003).

[53] T. R. de Oliveira, G. Rigolin, and M. C. de Oliveira, Phys. Rev. A **73**, 010305(R) (2006); Phys. Rev. A **74**, 039902 (2006); Phys. Rev. A **75**, 039901 (2007); T. R. de Oliveira, G. Rigolin, M. C. de Oliveira, and E. Miranda, Phys. Rev. Lett. **97**, 170401 (2006); S. M. Giampaolo and B. C. Hiesmayr, Phys. Rev. A **88**, 052305 (2013). Z.-Y. Sun, Y. -Y. Wu, J. Xu, H. -L. Huang, B. -F. Zhan, B. Wang, and C.-B. Duan, Phys. Rev. A **89**, 022101 (2014).

[54] M. Schechter and P. C. E. Stamp, Phys. Rev. B **78**, 054438 (2008), and references therein.

[55] J. Struck, C. Ölschläger, R. Le Targat, P. Soltan-Panahi, A. Eckardt, M. Lewenstein, P. Windpassinger, and K. Sengstock, Science **333**, 996 (2011); J. Simon, W. S. Bakr, R. Ma, M. E. Tai, P. M. Preiss, and M. Greiner, Nature (London) **472**, 307 (2011), and references therein.

[56] J. -J. García-Ripoll and J. I. Cirac, New. J. Phys. **5**, 76 (2003); L. -M. Duan, E. Demler, and M. D. Lukin, Phys. Rev. Lett. **91**, 090402 (2003), and references therein.

[57] X. -L. Deng, D. Porras, and J. I. Cirac, Phys. Rev. A **72**, 063407 (2005). H. Häffner, C. Roos, and R.Blatt, Phys. Rep. **469**, 155 (2008); K. Kim, M.-S. Chang, S. Korenblit, R. Islam, E. E. Edwards, J. K. Freericks, G.-D. Lin, L.-M. Duan, and C. Monroe, Nature (London) **465**, 590 (2010); R. Islam, E. E. Edwards, K. Kim, S. Korenblit, C. Noh, H. Carmichael, G.-D. Lin, L.-M. Duan, C.-C. Joseph Wang, J. K. Freericks, and C. Monroe, Nature Commun. **2**, 377 (2011); J. Struck, M. Weinberg, C. Ölschläger, P. Windpassinger, J. Simonet, K. Sengstock, R. Höppner, P. Hauke, A. Eckardt, M. Lewenstein, and L. Mathey, Nature Physics **9**, 738 (2013), and references therein.

[58] L. M. K. Vandersypen and I. L. Chuang. Rev. Mod. Phys. **76**, 1037 (2005); J. Zhang, M.-H. Yung, R. Laflamme, A. Aspuru-Guzik, J. Baugh, Nature Communications **3**, 880 (2012); K. Rama Koteswara Rao, H. Katiyar, T. S. Mahesh, A. Sen(De), U. Sen, and A. Kumar, Phys. Rev. A **88**, 022312 (2013), and references therein.

[59] H. Nishimori, AIP Conf. Proc. **248**, 269 (1991).

[60] T. Chanda, T. Das, D. Sadhukhan, A. K. Pal, A. Sen De, and U. Sen, Phys. Rev. A **92**, 062301 (2015)

[61] S. -J. Gu, H. -Q. Lin, and Y. -Q. Li, Phys. Rev. A **68**, 042330 (2003); O. F. Syljuasen, Phys. Rev. A **68**, 060301 (2003).